Forces shaping a Hox morphogenetic gene network

Sol Sotillos[1], Mario Aguilar[1], and James Castelli-Gair Hombría[2]

Centro Andaluz de Biología del Desarrollo, Consejo Superior de Investigaciones Científicas, Junta de Andalucía, Universidad Pablo de Olavide, 41013 Seville, Spain

Edited by Matthew P. Scott, Howard Hughes Medical Institute and Stanford University, Stanford, CA, and approved January 24, 2013 (received for review July 30, 2012)

The Abdominal-B selector protein induces organogenesis of the posterior spiracles by coordinating an organ-specific gene network. The complexity of this network begs the questions of how it originated and what selective pressures drove its formation. Given that the network likely formed in a piecemeal fashion, with elements recruited sequentially, we studied the consequences of expressing individual effectors of this network in naive epithelial cells. We found that, with exception of the Crossveinless-c (Cv-c) Rho GTPase-activating protein, most effectors exert little morphogenetic effect by themselves. In contrast, Cv-c expression causes cell motility and down-regulates epithelial polarity and cell adhesion proteins. These effects differ in cells endogenously expressing Cv-c, which have acquired compensatory mechanisms. In spiracle cells, the down-regulation of polarity and E-cadherin expression caused by Cv-c–induced Rho1 inactivation are compensated for by the simultaneous spiracle up-regulation of guanine nucleotide exchange factor (GEF) proteins, cell polarity, and adhesion molecules. Other epithelial cells that have coopted Cv-c to their morphogenetic gene networks are also resistant to Cv-c's deleterious effects. We propose that cooption of a novel morphogenetic regulator to a selector cascade causes cellular instability, resulting in strong selective pressure that leads that same cascade to recruit molecules that compensate it. This experimental-based hypothesis proposes how the frequently observed complex organogenetic gene networks are put together.

evolution | morphogenesis | homeotic gene | realizator gene | signaling

Organogenesis is directed by the activation of gene regulatory networks in specific positions of the embryo. In *Drosophila,* well-studied models include the posterior spiracles, in which the organogenesis gene network is activated downstream of the Hox selector protein Abdominal-B (Abd-B) (1); the salivary glands, in which the network is activated by Sex combs reduced (Scr) (2); and the trachea, in which the network is activated by Trachealess (Trh) and Ventral veinless (Vvl) (3). Although these three organs are morphologically and functionally different, in all a complex gene network of intermediate transcription factors and signaling molecules modulates a similar combination of cell adhesion, cell polarity, and cytoskeleton realizators.

Considering that these gene networks likely formed in a piecemeal fashion, with elements of the network recruited sequentially during organ evolution, two different scenarios can be envisaged. In one of these scenarios, the selective pressure to recruit each of the elements of the cascade is driven entirely by external environmental factors. In the other scenario, although an external selective pressure might have acted as the initial trigger for organ formation, endogenous physiological and developmental constraints would have been used later to shape the network by influencing what is developmentally stable and what is not.

Using morphogenesis of the posterior spiracles as a model, in this work we studied how the activity of particular genes in the Abd-B network affects epithelial cell behavior and how this may have influenced the modulation of other existing genes of the network or even resulted in the recruitment of new genes into it.

Results and Discussion

The downstream effectors of the Abd-B posterior spiracle cascade include the RhoGTPase regulators RhoGEF64C, RhoGEF2, and the RhoGAP Crossveinless-c (Cv-c), which control the cytoskeletal organization during spiracle morphogenesis (1, 4, 5) (Fig. 1*A*). The cascade also activates various nonclassical cadherins, stabilizes the protein levels of epithelial cadherin (E-Cad), and up-regulates the transcription of the apical cell polarity determinant Crumbs (Crb) (1) (Fig. 1*A*).

To investigate the contributions of these effectors to spiracle morphogenesis, we expressed each effector individually in epithelial cells in which they normally are not expressed or are expressed a lower levels than in the spiracle. This was achieved using either the epithelial ubiquitous *69B-Gal4* driver or the posterior compartment-specific *engrailed-Gal4* (*en-Gal4*) line to activate the different genes under the control of the upstream activation sequence (UAS). We found that individual expression of RhoGEF2, RhoGef64C, E-Cad, Cadherin 74A (Cad74A), or Cadherin 86C (Cad86C) had little effect on epithelial cell behavior (Fig. 1 *B–F*, arrowheads), but Cv-c RhoGAP or Crb expression resulted in strong effects on epithelial cell behavior (Fig. 1*G*, arrowhead). Crb is a key determinant of apical polarity, and its overexpression has been shown to interfere with apicobasal polarity, resulting in tissue collapse. Because Crb-induced effects are unrelated to normal tissue morphogenesis, we did not study them further in this work.

Cv-c is a RhoGAP protein required for Rho1-mediated actin reorganization (6, 7) that is activated transcriptionally in several morphogenetically active epidermal tissues, including leading edge cells during embryo dorsal closure, salivary gland primordia, tracheal pits, and invaginating posterior spiracles (6) (Fig. S1*A*). Given that *cv-c* mutations result in morphogenetic abnormalities in all of these tissues (6, 8, 9), we examined in detail this important epithelial morphogenetic regulator and its interactions with other downstream effectors of the Abd-B spiracle cascade.

Analysis of Ectoderm Epithelial Behavior Induced by *cv-c* Expression. To study the cellular morphogenetic effects controlled by this RhoGAP, we expressed *cv-c* ectopically in the posterior compartment of each segment from stage 11 onward using the *en-Gal4* line (Fig. S1 *B* and *C*). This allowed us to compare the shape and behavior of the normal nonexpressing anterior compartment cells with those of neighboring posterior compartment cells in which we induced Cv-c. Expression of Cv-c or Cv-c fused to a C-terminal Venus green fluorescent protein (GFP) tag induced similar effects, and were used indiscriminately. As a negative control, we expressed a Cv-c^{R601Q}-GFP protein, in which the critical catalytic arginine 601 in the GTPase-activating protein (GAP) domain is mutated to glutamine. This mutation is present in the *cv-c*^{7} allele, which produces an inactive protein (6).

Expression of Cv-c^{R601Q}-GFP did not affect the cell shape or subcellular localization of ectodermal proteins such as atypical PKC (aPKC), Crb, E-Cad, Discs large (Dlg), and Scribble. These embryos developed into normal adult flies, indicating that

Author contributions: S.S., M.A., and J.C.-G.H. designed research; S.S. and M.A. performed research; S.S., M.A., and J.C.-G.H. analyzed data; and S.S. and J.C.-G.H. wrote the paper.

The authors declare no conflict of interest.

This article is a PNAS Direct Submission.

[1]S.S. and M.A. contributed equally to this work.

[2]To whom correspondence should be addressed. E-mail: jcashom@upo.es.

This article contains supporting information online at www.pnas.org/lookup/suppl/doi:10.1073/pnas.1212970110/-/DCSupplemental.

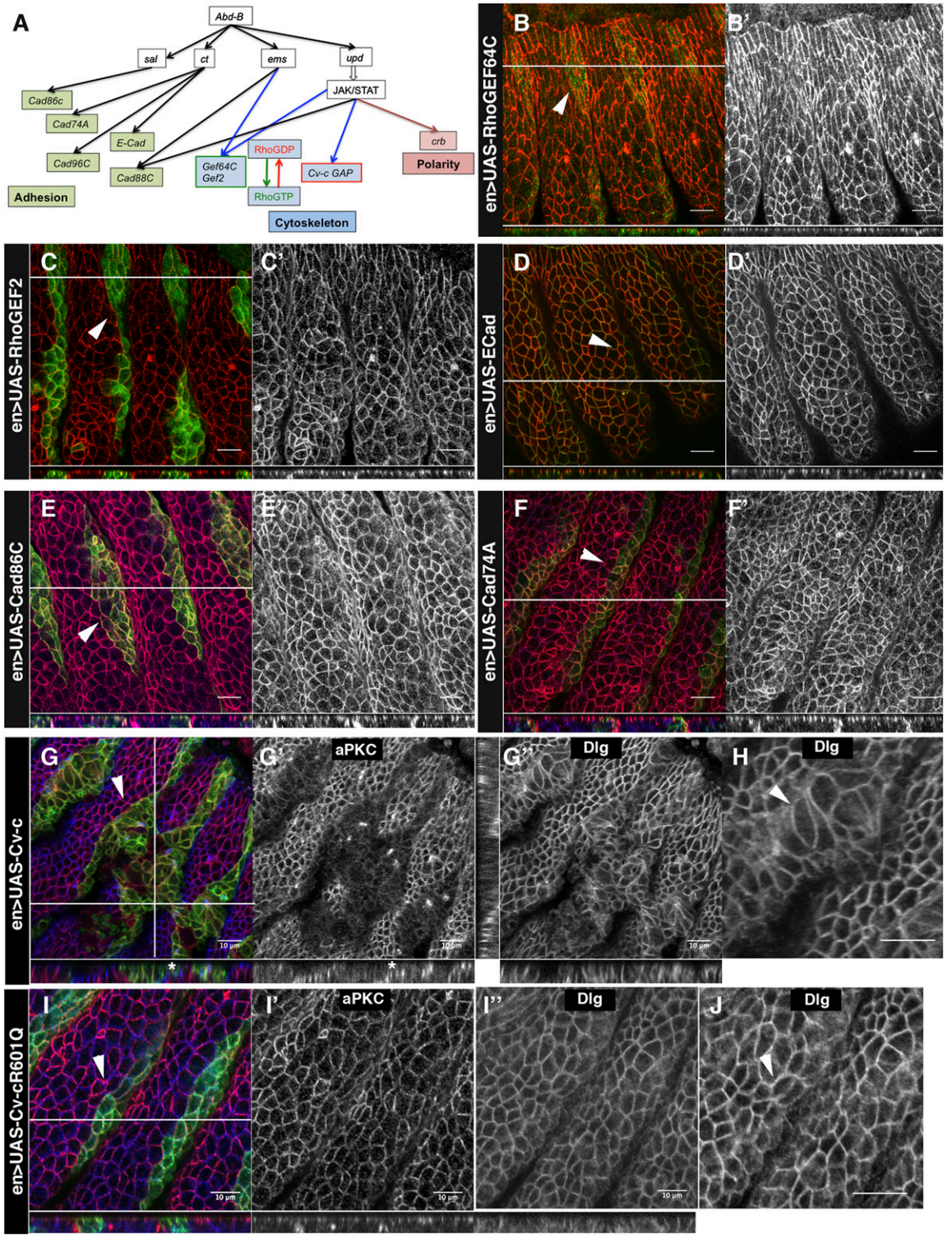

Fig. 1. Epithelial cell behavior after expression of single Abd-B effectors. (*A*) Schematic representation of the Abd-B posterior spiracle regulatory cascade and its downstream effectors. (*B–J*) Epidermis of stage 14–15 *Drosophila* embryos in which the indicated effector was expressed using *en-Gal4*. In all color panels, the cells expressing the effector are labeled in green. (*B*) RhoGEF64C expression (green) does not affect cell shape or apical polarity markers (aPKC in *B′* and red in *B*). (*C*) Epidermal cells expressing RhoGEF2 have deeper segment grooves, but the cells maintain position and polarity markers (aPKC in red and in *C′*). (*D–F*) Expression of E-Cad (*D*), Cad86C (*E*), or Cad74A (*F*) has no obvious effect on cell behavior, aPKC membrane localization (red in *D*, *D′*, *E*, *E′*, *F*, and *F′*), or Dlg (blue in *D*, *E*, and *F*). (*G*) Cv-c expression in epithelial cells that normally do not express it causes loss of the apical marker aPKC (*G′* and red in *G*), with little effect on the basolateral marker Dlg (*G″* and blue in *G*). (*H*) Close-up of *G″*; the arrowhead indicates Cv-c–expressing cells with changed shape. (*I*) Expression of inactive Cv-c^{R801Q} (green) in the epidermis does not affect cell shape or polarity, as shown by staining with anti-aPKC (*I′* and red in *I*) and anti-Dlg (*I″* and blue in *I*). (*J*) Close-up of *I″*; the arrowhead indicates cells expressing Cv-c^{R801Q}. Below most panels is a Z-section taken across the region indicated by the thin white line. In color panels, aPKC is red, GFP is green, and Dlg is blue. Anterior is left, and dorsal is up. Arrowhead points at cells expressing the effector indicated in the panel. (Scale bars: 10 μm.)

Cv-c^{R601Q}-GFP does not interfere with the endogenous Cv-c function (Fig. 1*I*, arrowhead; see Fig. 3*B*). In contrast, expression of *UAS-cv-c* or *UAS-cv-c-GFP* driven by *en-Gal4* results in lethality. In these embryos, the Cv-c–expressing cells change shape, becoming up to 50% wider (Fig. 1*G″* and *H*; compare with Fig. 1*I″* and *J*; quantified in *SI Materials and Methods*). In many cases, stripes of Cv-c–expressing cells from adjacent segments fuse, indicating that they either have increased motility or can displace the neighboring WT cells; 19 of 48 *en-Gal4 > UAS-Cv-c* embryos exhibited at least one segment fusion (Figs. 1*G* and 3*A*, *Lower*). Cv-c–expressing cells also exhibited a strong down-regulation of the apical polarity proteins aPKC and Crb (Fig. 1*G*) and the adherens junction proteins E-Cad and β-catenin (Fig. 3*C*), but had little effect on expression levels of the basolateral septate junction markers Dlg, Scribble, and Coracle (Figs. 1 *G″* and *H* and 3*C*).

Because Cv-c has been shown to inactivate Rho1 (4, 7, 10, 11), we tested whether the observed phenotypes were mimicked by Rho1 inactivation. Expression of the dominant negative Rho^{N19} with *en-Gal4* resulted in phenotypes comparable to those seen with expression of Cv-c-GFP (Fig. 2*B* and Fig S2*E*). Simultaneous expression of Cv-c-GFP and activated Rho1^{V14} rescued the loss of aPKC, Crb, and E-Cad (Fig. 2*D*) and restored normal cell shape and the cuticle defects caused by Cv-c (Fig S2*C*). In contrast, an activated form of Rac did not rescue the phenotypes caused by Cv-c, and overexpression of a dominant negative Rac did not affect apical polarity protein distribution (Fig. S3), confirming the specificity of Cv-c for Rho1. These results indicate that the cell behaviors induced by ectopic Cv-c expression in the ectoderm are related to its expected function as a down-regulator of Rho1 activity.

The loss of E-Cad and apical markers on expression of either Cv-c or Rho^{N19} did not cause massive cell death, as demonstrated by the continuous presence of GFP-expressing cells during embryogenesis and the modest levels of caspase-3 activity detected in these embryos (Fig. 2*E*). Accordingly, the phenotypes caused by Cv-c are not recovered by coexpression of the *Drosophila* inhibitor of apoptosis protein 1 (DIAP1) (12) (Fig. 2*F*).

The foregoing results indicate that recruitment of Cv-c to ectoderm epithelial cells has strong morphogenetic consequences, possibly explaining why it is transcriptionally activated in so many actively rearranging epithelial cells.

Motile Behavior of Cv-c–Expressing Cells. To understand how Cv-c expression in the posterior compartment causes segment fusions, we studied the embryos in vivo and reconstructed the 3D organization of their epithelia. We found that the *en-Gal4* line drives expression in the posterior compartment of each segment, and every stripe is separated from those in other segments by anterior cells (Fig. 3*A*, *Upper* and Movie S1). Stripes of cells expressing the mutated Cv-c^{R601Q} protein were clearly separated from one another during development (Figs. 1*I* and 3*B*). In contrast, in *en-Gal4>UAS-cv-c-GFP* embryos, the Cv-c-GFP–expressing cells exhibited greater motility, which can result in the occasional fusion of *en-Gal4*–expressing stripes (Fig. 3*A*, *Lower* and Movie S2). The Cv-c–expressing cells maintained tissue coherence, indicating that these cells maintain cell adhesion despite the observed E-Cad down-regulation (Fig. 3*C*). Whereas the motility of these cells is likely caused by Cv-c overexpression, the segment fusion may be independent of Cv-c, given that posterior cells have similar affinities that may lead to posterior compartment merger once in contact (13).

A 3D analysis of fused segments revealed that the Cv-c–expressing cells "crawled" over the anterior compartment cells that remained beneath them (Figs. 1*G* and 3 *C* and *C′*, asterisks).

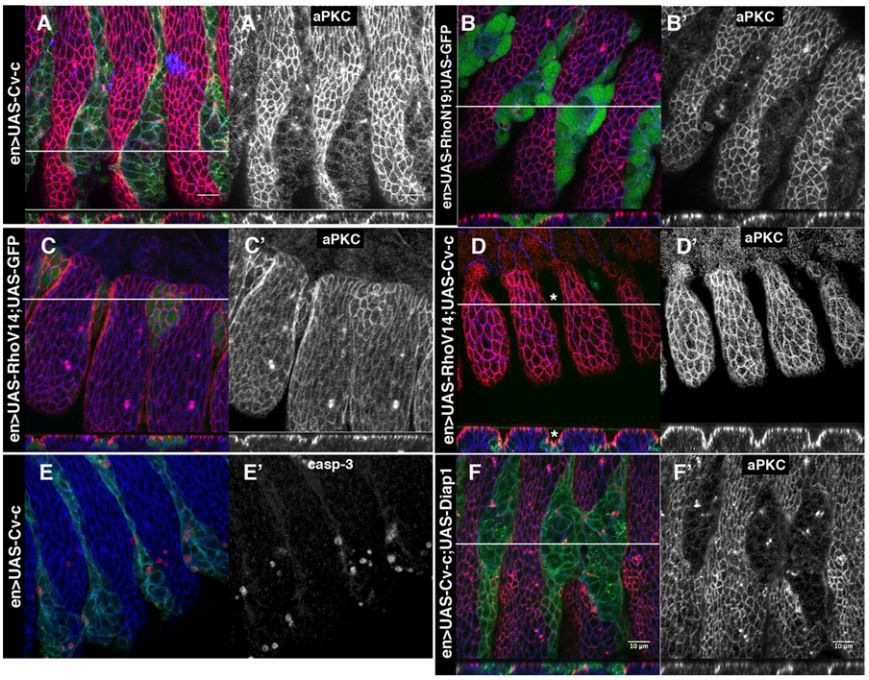

Fig. 2. Effect of Cv-c and Rho1 expression on epithelial cell behavior. (*A*–*F*) Epidermis of stage 14–15 *Drosophila* embryos in which the indicated constructs were expressed using *en-Gal4*. (*A*) Cv-c expression in epithelial cells that normally do not express it causes loss of aPKC (*A′*). (*B*) Expression of the dominant negative Rho1^{N19} causes the same defects on aPKC expression (red in *B* and *B′*). (*C*) Expression of an active Rho1^{V14} results in exaggerated segmental grooves but does not affect apical markers (aPKC; *C′* and red in *C*). (*D*) Expression of Rho1^{V14} rescues the loss of apical cell polarity caused by Cv-c expression. Note that the apparent areas without aPKC expression (asterisks in *D*) are due to the exaggerated segmental grooves present in these embryos, as seen in the Z-section shown below *D′*. (*E* and *F*) Defects caused by ectopic Cv-c are not due to cell death, given that Cv-c expression persists with only moderately increased cell death, as shown by anti-active caspase 3 staining (activated caspase 3 in *E′* and red in *E*), and the phenotypes caused by Cv-c induction cannot be rescued by coexpression of the apoptosis inhibitor Diap1 (*F*, aPKC in red and GFP in green). Note the occasional segment fusions. Dlg is shown in blue in *A*–*F*. Below most panels is a Z-section taken across the thin white line. Anterior is left, and dorsal is up. (Scale bars: 10 μm.)

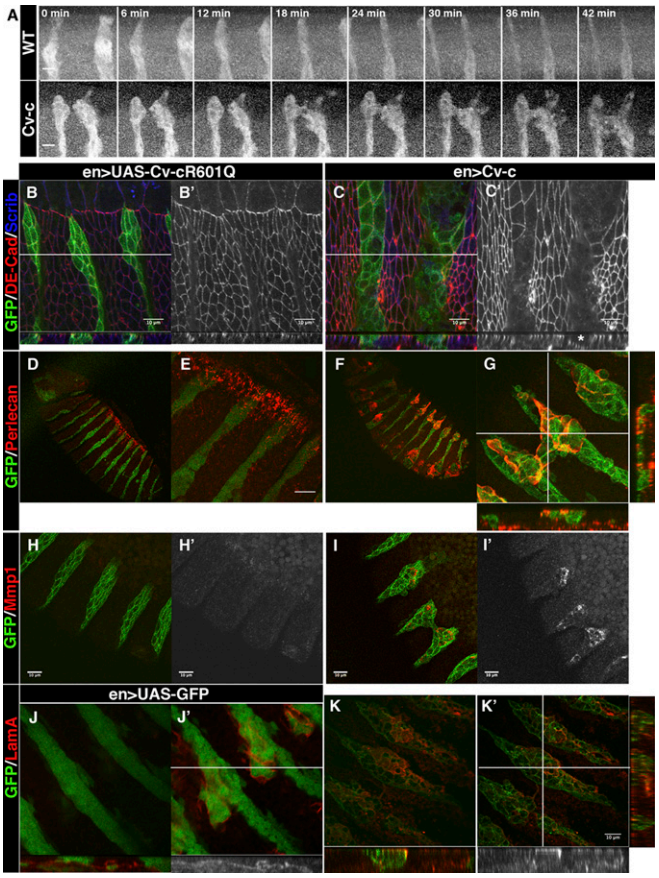

Fig. 3. Expression of Cv-c induces epithelial reorganization. (*A*) Stills from a time-lapse movie showing the cell behavior of engrailed cells expressing GFP (*Upper*) or Cv-c (*Lower*) during embryonic development. Whereas WT cells maintain their position in the posterior of the segment, Cv-c–expressing cells can move as a coherent tissue, in some cases fusing to the neighboring *engrailed* stripe. (*B–M*) Epidermis of stage 14 embryos in which the indicated UAS lines were expressed using *en-Gal4* as a driver. (*B*) Epidermal cells expressing inactive Cv-c^{R601Q} in the posterior compartment are distributed as a monolayer. E-Cad is shown in red; Scribble, in blue. (*C*) Posterior cells expressing Cv-c crawl over adjacent WT cells (Note that in *C′*, the Cv-c–expressing cells have down-regulated E-Cad and are moving over the WT anterior cells that still express normal levels of E-Cad, denoted by an asterisk.) E-Cad is in shown red; Scribble, in blue. (*D* and *E*) In control Cv-c^{R601Q}–expressing embryos, Perlecan (shown in red) localizes to the mesoderm and along the cells going through dorsal closure. GFP is in green. (*F* and *G*) Motile cells expressing Cv-c are surrounded by Perlecan (shown in red). (*H* and *I*) Expression of Mmp1 metalloprotease in control and Cv-c–expressing embryos (*H′* and *I′* and red in *H* and *I*). GFP is in green. (*J* and *K*) Expression of laminin A (shown in red) in control (*J*) and Cv-c expressing embryos (*K*). Sections through the ectoderm (*J* and *K*) and mesoderm (*J′* and *K′*) levels are shown. GFP is in green. In *B*, *C*, *G*, *J*, and *K*, Z-sections are shown along the thin white lines. (Scale bars: 10 μm.)

Unlike control embryos (Fig. 3 *D* and *E*), the motile Cv-c cells were surrounded by high levels of the heparan sulfate proteoglycan perlecan (Fig. 3 *F* and *G*), expressed ectopically the Mmp1 metalloprotease (Fig. 3*I*; compare with Fig. 3*H*), and up-regulated the expression of laminin A (Fig. 3*K*; compare with Fig. 3*J*). These results show that Cv-c cells move cohesively over a newly formed extracellular matrix.

Tissue-Specific Effects of Cv-c Expression. We have shown that in the embryonic epithelium, the specific Rho1 down-regulation mediated by the RhoGAP activity of Cv-c disrupts the normal levels of E-Cad and apical polarity proteins. Rho1 inactivation has been shown to cause similar effects in the eye epithelium, which has been linked to the need for Rho1 to maintain adherens junctions during epithelial remodeling (14). Although we agree with this interpretation, we find our results puzzling, given the presence of E-Cad, Crb, and aPKC at high levels in the epithelial cells in which *cv-c* is normally expressed (Fig. S1*A*; compare with Fig. S1 *D*, *K*, and *Q*) (1, 15, 16). To test whether the defects that we observed can be explained by the Gal4 system expressing unusually high Cv-c levels with respect to endogenous expression, we examined the effects caused by Gal4-induced Cv-c overexpression in the tissues expressing endogenous Cv-c. Even when overexpressing Cv-c with the spiracle-specific line *ems-Gal4*, the ectopic Cv-c was unable to down-regulate E-Cad, aPKC, or Crb in the posterior spiracles (Fig. 4*B*; compare with Fig. 4*A*). Similarly, ectopic Cv-c in cells of the leading edge (Fig. 4*C*), trachea (Fig. 4*D*), or salivary glands (Fig. 4*E*) did not cause down-regulation of apical markers or E-Cad. This finding is particularly evident in the experiment using the *en-Gal4* line, in which identical levels of Cv-c-GFP in the posterior compartment down-regulated epithelial markers from all posterior compartment cells except those of the leading edge, which express Cv-c endogenously (Fig. 4*C*, arrowheads; quantified in Fig. S4). These data imply that the epithelial tissues that normally express *cv-c* respond differently to Cv-c, suggesting that they have compensatory mechanisms that allow the local down-regulation of Rho1 without the loss of apical polarity and adhesion properties.

Abd-B Recruitment of Compensatory Mechanisms of Posterior Spiracles. In the posterior spiracles, Abd-B activated not only *cv-c*, but also various cadherins and polarity genes (Fig. 1*A*). Of particular interest is the finding that despite the ubiquitous expression of *crb* in all ectoderm cells, the Abd-B cascade reinforces *crb* transcription through a spiracle-specific enhancer (1). To evaluate whether the increased Crb levels and cell adhesion protein up-regulation in spiracles could be part of the compensatory mechanism, we tested whether embryos heterozygous for these genes became more sensitive to Cv-c levels. Expression of Cv-c in the spiracles of *crb* heterozygous mutants resulted in spiracles with frequent invagination defects and abnormal expression of polarity molecules (Fig. 4*H*), with 28% (n = 53) of *crb* heterozygous embryos overexpressing Cv-c demonstrating spiracle defects. In contrast, the Cv-c^{R601Q} protein had no effect (n = 84) (Fig. 4*F*). The same phenomenon was seen in a heterozygous mutant background for *E-cad* (33%; n = 109) (Fig. 4*I*), *aPKC* (23%; n = 71), RhoGef64C (20%; n = 66), or RhoGEF2 (24%; n = 55), all of which were modulated by the Abd-B cascade in the posterior spiracles.

To investigate whether the Abd-B posterior spiracle gene network includes compensatory mechanisms to ameliorate the effects of Cv-c on polarity and adhesion, we ectopically expressed Cv-c and Abd-B simultaneously. We found that expression of Abd-B rescued Cv-c epithelial defects in the areas associated with formation of ectopic spiracles (Fig. 4 *L* and *M*). Similarly, we found that ectopic expression of Abd-B was also capable of rescuing the defects caused by Rho1DN expression (Fig. S5).

These results indicate that Abd-B controls a gene network in the posterior spiracles that activates both Cv-c and the compensatory mechanism, restricting the defects caused by Cv-c in the epithelium.

Compensation for Cv-c–Induced Defects by Expression of Various Cell Proteins. The foregoing data suggest that some of the posterior spiracle Abd-B targets can compensate for the defects caused by down-regulation of Rho by Cv-c. To identify targets with a possible compensatory effect, we tested whether expression of any of the Abd-B spiracle effectors could rescue the defects caused by Cv-c in the epidermis.

GAP and GEF proteins have opposing regulatory effects on Rho1 activation. Although both RhoGEF2 and RhoGEF64C have been shown to function in the spiracle under the control of Abd-B, only RhoGEF2 expression was able to recover the membrane localization of both E-Cad (blue in Fig. 5*A*; asterisks

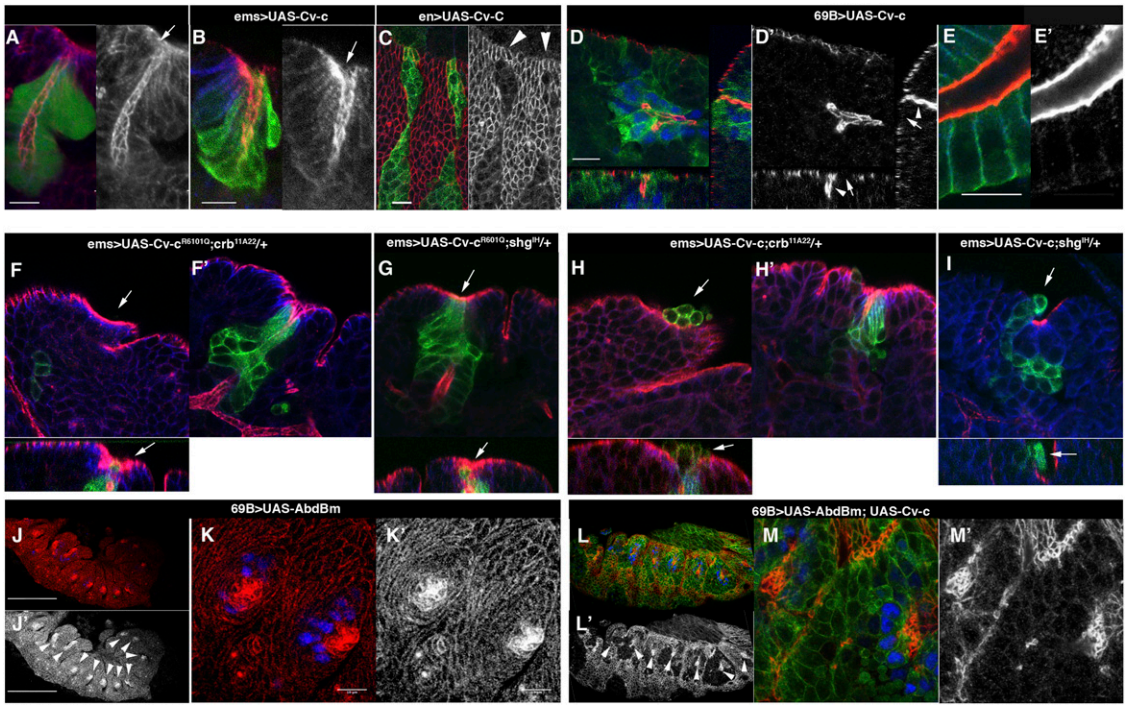

Fig. 4. Tissue-specific response to Cv-c activation. (*A–E*) Epidermal cells that normally express Cv-c do not lose apical polarity markers as a result of increased Cv-c expression. Apical is labeled with aPKC in red and basolateral in blue with either Dlg (*A*, *C*, and *E*) or neurotactin (*B*). (*A*) WT stage 16 embryo expressing GFP (green) driven by the spiracle-specific *ems-Gal4* line. (*B*) Spiracle cells overexpressing Cv-c with *ems-Gal4* show normal aPKC and neurotactin expression. GFP staining is less conspicuous in *B* than in *A* because of the membrane location of Cv-c-GFP. Arrows indicate the apical region in the posterior spiracles. (*C*) Epidermal cells expressing Cv-c using *en-Gal4* as a driver lose aPKC, except those of the leading edge (arrowheads). (*D*) Tracheal cells, labeled with anti-Trh (blue nuclei), do not lose aPKC (red) after Cv-c ectopic expression (arrowheads; compare with the decrease in nearby ectodermal cells, indicated by the arrow). (*E*) Salivary gland cells do not lose aPKC localization after Cv-c ectopic expression. (*F–I*) Ectopic posterior spiracle Cv-c expression in heterozygous *crb* or *E-cad* embryos. Posterior spiracles of heterozygous mutants for *crb* (*F* and *H*) or the *E-cad* allele shg^{IH} (*G* and *I*) develop normally in control embryos expressing the mutant Cv-c^{R601Q} (*F* and *G*), but frequently exhibit invagination defects when expressing WT Cv-c (*H* and *I*). In *H* and *I*, arrows indicate spiracle cells that failed to invaginate and do not express aPKC and the homologous spiracle region in embryos expressing the mutated Cv-c form in *F* and *G*. *F* and *F′* and *H* and *H′* show two confocal sections of the same spiracle at different focal planes. (*J*) Ectopic Abd-B expression driven in the ectoderm with the *69B-Gal4* line forms supernumerary posterior spiracles (arrowheads), as detected with anticut (Ct) expression (blue), without affecting the cell polarity (aPKC in red or gray; note the increased levels of aPKC in the spiracle lumen). (*K*) Close-up of *J* showing the ectopic spiracles formed in two segments. (*L*) Embryo expressing Cv-c and Abd-B simultaneously with the *69B-Gal4* line. Note the loss of aPKC from the anterior trunk segments except in the areas associated with formation of ectopic posterior spiracles (blue, Ct expression in the ectopic spiracles; green, Cv-c–expressing cells; red or gray, aPKC). (*M*) Close-up of *L* showing that aPKC expression remains associated with the ectopic posterior spiracles (arrowheads). In all panels, dorsal is up and anterior is left. (Scale bars: 10 μm in *A–E* and *K*; 100 μm in *J*.)

in Fig. 5*A′*) and aPKC (blue in Fig. 5*B*; asterisks in Fig. 5*B′*). In our experiments, RhoGEF64C did not localize to the membrane when expressed in the trunk with *en-Gal4*, whereas RhoGEF2 did localize, possibly explaining why only RhoGEF2 was capable of compensating for Cv-c defects in the epithelium.

We also tested whether the outcome of Cv-c activation could be normalized by coexpression of E-Cad or aPKC, which are upregulated in the posterior spiracles (Fig. S1). When aPKC (a major regulator of apical polarity) was coexpressed with Cv-c, both aPKC (Fig. 5*C*, blue) and E-Cad (Fig. 5*C*, red; Fig. 5*C′*) localization to the membrane were recovered (Fig. 5*C′*, arrowhead and asterisk). However, when E-Cad and Cv-c were coexpressed, only E-Cad membrane localization was restored, whereas aPKC localization remained cytoplasmic (red in Fig. 5*D*; arrowhead and asterisk in Fig. 5*D′*).

The foregoing results showing that newly transcribed and translated E-Cad can localize normally to the membrane in Cv-c–expressing cells suggest that Cv-c may be perturbing E-Cad membrane recycling, a fundamental mechanism in normal development (17). In agreement with this idea, we did not detect high *E-cad* RNA expression levels in posterior spiracles despite the high E-Cad protein levels observed, suggesting greater E-Cad stability or increased recycling in the spiracles.

To test whether increased endocytic membrane recycling could compensate for some of the defects, we coexpressed Cv-c with the endocytic regulator Rab11. In this situation, E-Cad and aPKC localization are strongly normalized in the dorsal region (arrowheads in Fig. 5*E*; asterisks in Fig. 5*E′* and *E″*). Interestingly, we found higher Rab11 levels in the WT posterior spiracles compared with neighboring tissues (Fig. 5*F*, arrowhead). Abd-B was required for the increased spiracle Rab11 protein levels, given that these disappeared in *Abd-B* mutant embryos, and ectopic Abd-B expression resulted in ectopic Rab11 levels in anterior segments (Fig. 5 *G* and *H*, arrowheads). Moreover, in ectopically expressing Cv-c embryos, the rescue in polarity caused by ectopic Abd-B expression was correlated with the appearance of higher levels of E-Cad and Rab11 in the areas of ectopic spiracle formation (Fig. S6).

The foregoing results indicate that ectoderm expression of Cv-c causes cell polarity defects that can be compensated for by reinforcing the expression of apical polarity components through either increased recycling or transcription. Our observation that in the spiracles, Abd-B controls the levels of proteins capable of rescuing Cv-c defects in the ectoderm explains why Abd-B can compensate for Cv-c epithelial defects.

Contribution of Cv-c to Shaping of Organogenesis Networks. Organogenesis of the salivary glands, trachea, and posterior spiracles is induced by the Scr, Trh/Vvl, and Abd-B selector proteins, respectively (1–3, 18). Although the networks activated by these transcription factors differ significantly, they share common

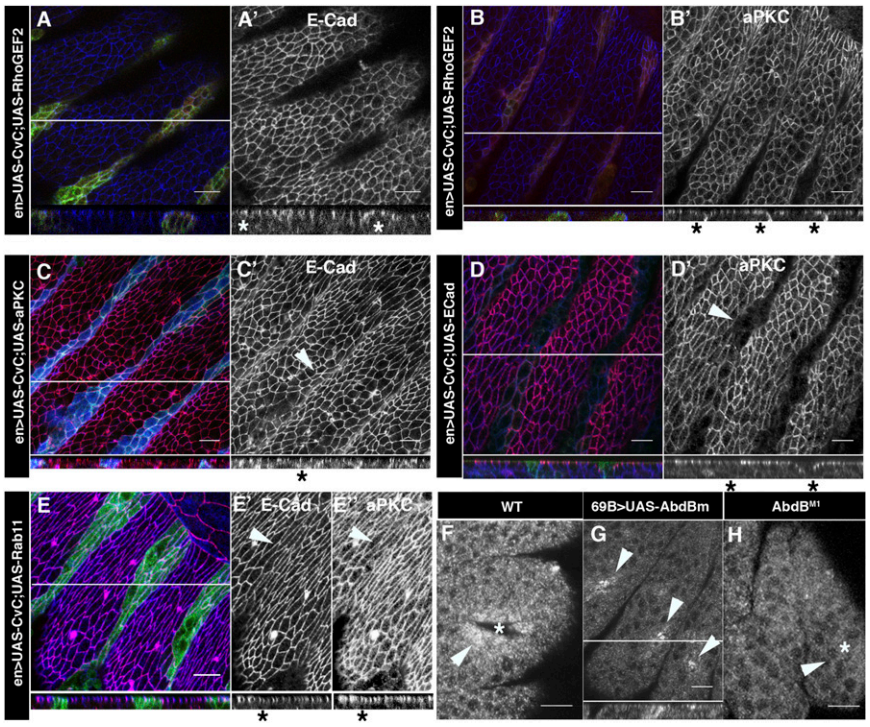

Fig. 5. Rescue of Cv-c–induced polarity defects. (*A*–*D*) Rescue of apically polarized protein localization in cells expressing Cv-c and Abd-B effectors. (*A* and *B*) Coexpression of RhoGEF2 (red in *A* and *B*) restores both E-Cad localization (*A*′ and blue in *A*) and aPKC (*B*′ and blue in *B*). (*C*) Expression of an aPKC-myc–tagged protein in ectodermal cells restores aPKC (blue in *C*) and E-Cad membrane localization (*C*′ and red in *C*). (*D*) Expression of E-Cad is unable to restore aPKC membrane localization (*D*′ and red in *D*). (*E*) Both E-Cad and aPKC membrane localization are rescued when Cv-c is coexpressed with Rab11 (red and blue in *E*, and *E*′ and *E*″). (*F*–*H*) Increased Rab11 levels in the posterior spiracle depend on Abd-B. (*F*) Cross-section of a posterior spiracle (asterisk) in a WT embryo shows higher protein levels of Rab11 in spiracle cells compared with neighboring cells (arrowhead). (*G* and *H*) Ectopic Abd-B expression with *69B-Gal4* increases Rab11 in all trunk segments (*G*, arrowheads), whereas increased Rab11 levels disappear in Abd-B mutant embryos (*H*; the asterisk marks the position in A8 where the spiracle normally forms). *A*–*E* and *G* show Z-sections along the thin white lines; the asterisk in these Z-sections indicates the cells overexpressing Cv-c. In all panels, dorsal is up and anterior is left. (Scale bars: 10 μm.)

targets, including *cv-c*, *crb*, and *E-cad*. Among these, *cv-c* has received the most attention, because it is regulated by transcriptional activation before the onset of morphogenetic movements and has the capacity to influence actin cytoskeleton organization through Rho1 regulation, and its mutation causes invagination defects in these tissues (4, 8, 9). Although published data indicate that Cv-c is required for normal invagination in these organs, our experiments indicate that by itself, Cv-c activation in the epithelium does not induce invagination, and that the resulting down-regulation of Rho1 has collateral effects on the maintenance of epithelial polarity and adhesion. We propose that during organ evolution, the cooption of Cv-c for cytoskeletal rearrangements leads to perturbation of epithelial maintenance, which requires the reinforcement of general polarity and adhesion molecules in those cells to compensate for the deleterious collateral defects. Thus, the recruitment of a new downstream morphogenetic regulator by a gene network can generate a selective pressure, leading that network to recruit other genes or to modify the expression of existing network genes to regain homeostasis. In the spiracles, this was achieved through de novo local transcriptional up-regulation of *crb*, various cadherins, and GEF regulators, as well as stabilization of E-Cad and Rab11, among other proteins, by the Abd-B cascade (1). *crb* up-regulation was also observed in the trachea and salivary glands (1, 15, 16) (Fig. S1), suggesting that a similar process might have occurred downstream of Scr and Trh. We believe that such pressures occur frequently during organ evolution, leading to the local modulation of proteins required for basic cell functions, which explains the frequent occurrence of tissue-specific enhancers in otherwise ubiquitously expressed genes.

Materials and Methods

Embryos grown at 25 °C were fixed for cuticle preparation and antibody staining using standard methods. A mutant Cv-c^{R601Q} and a WT C-terminal fusion to venus-GFP were generated and expressed using the *Gal4* system. Cell size quantification was performed, and in vivo time-lapse movies were recorded. Detailed information on procedures, mutants, constructs, and antibodies is provided in *SI Materials and Methods*.

ACKNOWLEDGMENTS. We thank S. Campuzano, H. Skaer, and B. Denholm for comments on the manuscript; Nicole Gorfinkield and J. Culi for advice on embryo filming and quantification; and D. Bilder, C. Dahmann, and P. Roth for reagents. This work was supported by the Spanish Ministerio de Investigación Ciencia e Innovación, Consolider, the European Regional Development Fund, and the Junta de Andalucía.

1. Lovegrove B, et al. (2006) Coordinated control of cell adhesion, polarity, and cytoskeleton underlies Hox-induced organogenesis in *Drosophila*. *Curr Biol* 16(22):2206–2216.
2. Panzer S, Weigel D, Beckendorf SK (1992) Organogenesis in *Drosophila melanogaster*: Embryonic salivary gland determination is controlled by homeotic and dorsoventral patterning genes. *Development* 114(1):49–57.
3. Boube M, Llimargas M, Casanova J (2000) Cross-regulatory interactions among tracheal genes support a co-operative model for the induction of tracheal fates in the *Drosophila* embryo. *Mech Dev* 91(1-2):271–278.
4. Simões S, et al. (2006) Compartmentalisation of Rho regulators directs cell invagination during tissue morphogenesis. *Development* 133(21):4257–4267.
5. Hu N, Castelli-Gair J (1999) Study of the posterior spiracles of *Drosophila* as a model to understand the genetic and cellular mechanisms controlling morphogenesis. *Dev Biol* 214(1):197–210.
6. Denholm B, et al. (2005) *crossveinless-c* is a RhoGAP required for actin reorganisation during morphogenesis. *Development* 132(10):2389–2400.
7. Sato D, Sugimura K, Satoh D, Uemura T (2010) Crossveinless-c, the *Drosophila* homolog of tumor suppressor DLC1, regulates directional elongation of dendritic branches via down-regulating Rho1 activity. *Genes Cells* 15(5):485–500.
8. Brodu V, Casanova J (2006) The RhoGAP *crossveinless-c* links *trachealess* and EGFR signaling to cell shape remodeling in *Drosophila* tracheal invagination. *Genes Dev* 20(13):1817–1828.
9. Kolesnikov T, Beckendorf SK (2007) 18 Wheeler regulates apical constriction of salivary gland cells via the Rho-GTPase-signaling pathway. *Dev Biol* 307(1):53–61.
10. Wong CM, Lee JM, Ching YP, Jin DY, Ng IO (2003) Genetic and epigenetic alterations of *DLC-1* gene in hepatocellular carcinoma. *Cancer Res* 63(22):7646–7651.
11. Healy KD, et al. (2008) DLC-1 suppresses non-small cell lung cancer growth and invasion by RhoGAP-dependent and independent mechanisms. *Mol Carcinog* 47(5):326–337.
12. Wang SL, Hawkins CJ, Yoo SJ, Müller HA, Hay BA (1999) The *Drosophila* caspase inhibitor DIAP1 is essential for cell survival and is negatively regulated by HID. *Cell* 98(4):453–463.
13. Jacinto A, et al. (2000) Dynamic actin-based epithelial adhesion and cell matching during *Drosophila* dorsal closure. *Curr Biol* 10(22):1420–1426.
14. Warner SJ, Longmore GD (2009) Distinct functions for Rho1 in maintaining adherens junctions and apical tension in remodeling epithelia. *J Cell Biol* 185(6):1111–1125.
15. Xu N, Keung B, Myat MM (2008) Rho GTPase controls invagination and cohesive migration of the *Drosophila* salivary gland through Crumbs and Rho-kinase. *Dev Biol* 321(1):88–100.
16. Letizia A, Sotillos S, Campuzano S, Llimargas M (2011) Regulated Crb accumulation controls apical constriction and invagination in *Drosophila* tracheal cells. *J Cell Sci* 124(Pt 2):240–251.
17. Nishimura T, Takeichi M (2009) Remodeling of the adherens junctions during morphogenesis. *Curr Top Dev Biol* 89:33–54.
18. Hombría JC, Lovegrove B (2003) Beyond homeosis—HOX function in morphogenesis and organogenesis. *Differentiation* 71(8):461–476.